

# Practical Considerations for Intra-Pulse Radar-Embedded Communications

Shannon D. Blunt and Casey R. Biggs  
EECS Dept. / Radar Systems Lab  
University of Kansas  
Lawrence, KS

**Abstract—** This paper examines some of the practical aspects of waveform design for intra-pulse radar-embedded communications. Specifically, the generation of communication waveforms at the tag is considered for the case when forward scatter (*i.e.* multipath) is present thus altering the received version of the radar waveform at the tag and potentially producing a mismatch between the tag and desired receiver. Also, because it may be difficult to precisely determine the exact temporal length of the incident radar waveform (especially when multipath is present), the communication waveform design process may employ a larger than necessary temporal extent to ensure the incident waveform is completely captured. The impact of this temporal expansion of the communication waveforms is considered where it has been found to actually improve performance (in the absence of multipath). As such a rule-of-thumb for the total expanded time-bandwidth product is determined as a function of observed symbol error rate performance.

## I. INTRODUCTION

For the intra-pulse radar-embedded communications configuration, a radar illuminates some region that contains a tag/transponder that will embed some message into the radar backscatter. This embedded message could be intended for the illuminating radar or some other receiver within the backscatter regime. The tag/transponder may operate anywhere from purely passive (harvesting energy only from the radar illumination) to active transmission that is triggered by the incident radar pulse. For all of these operational modes the tag (as we shall refer to it henceforth for simplicity) phase re-modulates the incident radar waveform into one of  $K$  different communication waveforms on an *intra*-pulse basis. The goal is thus to best design these communication waveforms such that they remain sufficiently hidden in the

radar backscatter (*i.e.* maintain low probability of intercept or LPI) while also being sufficiently dissimilar to one another so as to minimize the probability of communication error (*i.e.* the symbol error rate) on receive.

Previous work on radar-embedded communications has generally relied on either *inter*-pulse modulation or *intra*-pulse convolution. The former modulates on a pulse-to-pulse basis akin to a Doppler shift over numerous pulses (see, for example, [1-4]). While potentially availing quite good LPI properties, the data rate for such an approach is rather low (on the order of bits/second or bps). In contrast, the latter *intra*-pulse convolution-based approach [5] may enable very high data rates (on the order of Mbps). However, because it utilizes the same mathematical mechanism as physical scattering (namely a convolution operation), standard radar detection can be used to identify the embedded message thus greatly limiting LPI capabilities.

The *intra*-pulse modulation approach considered herein is a more recent addition to the pantheon of embedded-communications techniques. As described in [6, 7], this technique may potentially provide data-rates on the order of kbps or higher while likewise providing good LPI performance. The desired LPI characteristics are obtained by virtue of the fact that the communication signal is intentionally designed to possess a prescribed degree of similarity with the ambient radar scattering thus predicated the need for appropriate interference cancellation measures at the desired receiver (as well as knowledge of the set of expected communication waveforms). In this paper, some of the practical challenges of performing *intra*-pulse modulation are investigated.

## II. COMMUNICATION WAVEFORM DESIGN

Let us first consider the operation of determining the set of communication waveforms given a replica of the transmitted radar waveform. Presuming that sampling the radar waveform  $s(t)$  at its Nyquist rate of  $B$  samples/second produces a length  $N$  sampled version of the waveform, we

---

This work was sponsored under the Air Force Office of Scientific Research (AFOSR) Young Investigator Program.

shall over-sample by a factor of  $M$  to generate the vector  $\mathbf{s} = [s_0 \ s_1 \ \cdots \ s_{NM-1}]^T$  of length  $NM$ . The matrix

$$\mathbf{S} = \begin{bmatrix} s_{NM-1} & s_{NM-2} & \cdots & s_0 & 0 & 0 \\ 0 & s_{NM-1} & & s_1 & s_0 & 0 \\ & & \ddots & \vdots & \vdots & \ddots \\ 0 & 0 & & s_{NM-1} & s_{NM-2} & \cdots & s_0 \end{bmatrix} \quad (1)$$

of dimension  $NM \times (2NM-1)$  then represents the set of  $2NM-1$  possible delay shifts of the sampled waveform  $\mathbf{s}$  and thus contains generic information regarding the local ambient scattering (into which the communication waveform is to be embedded). The eigenvectors of  $\mathbf{S}\mathbf{S}^H$  are used to generate the  $K$  different communication waveforms. Because the radar waveform has been sampled  $M$  times higher than the Nyquist rate, the  $NM$  eigenvectors can be roughly partitioned into a set of  $N$  eigenvectors corresponding to large (or dominant) eigenvalues and the set of  $NM-N$  eigenvectors corresponding to small (or non-dominant) eigenvalues. The dominant and non-dominant eigenvector subspaces provide a mathematical representation for the ambient scattering akin to a “signal” subspace and “noise” subspace corresponding to the ambient radar scattering.

Previously in [6, 7], three methods were developed to generate the communication waveforms from the eigenvectors of  $\mathbf{S}\mathbf{S}^H$ . The Eigenvectors-as-Waveforms (EAW) approach uses  $K$  individual eigenvectors from the non-dominant subspace directly as each of the  $K$  communication waveforms. Alternatively, the Weighted Combining (WC) method uses  $K$  different known weight vectors to combine multiple eigenvectors from the non-dominant subspace to create the  $K$  communication waveforms. Finally, the Dominant Projection (DP) approach projects the dominant eigenvector subspace away from a known weight vector to generate the first communication waveform. The next communication waveform is then obtained by projecting the dominant space and the first communication waveform away from a second weight vector. This process is repeated for each of the  $K$  waveforms.

Because the ambient scattering acts as masking interference to the embedded communication waveforms, which are in turn designed according to the presumed eigenvector representation of the ambient scattering, the accuracy of the dominant and non-dominant eigenvectors and the way in which they are used directly impacts the overall symbol error rate performance. Since these eigenvectors are predicated upon a received replica of the transmitted radar waveform via (1), propagation effects may induce changes to the presumed radar waveform thereby producing a mismatch in the sets of eigenvectors at the tag and intended receiver. Such a mismatch may have quite deleterious consequences to

symbol error rate performance (even to the point of making reliable communication impossible).

An additional effect of multipath is the temporal expansion of the incident radar waveform (or at least what the tag presumes to be the radar waveform) due to delayed reception at the tag. A straightforward way in which to account for this effect is to “quantize” the temporal extent of the presumed radar waveform to a finite set of possible pulse widths where the selected pulse width is always greater (*i.e.* rounded up) than the presumed waveform termination. Of course, one possible outcome is mismatch (between tag and receiver) in the temporal extent of the resulting communication waveforms. This will be examined elsewhere though the reader should note that the Dominant Projection approach, previously found to be robust to sample offset effects [7], is negligibly affected by this source of mismatch.

Another result of expanded timewidth (beyond the nominal temporal extent of the radar pulse width) is that the communication waveform design procedure is afforded a higher dimensionality. This higher dimensionality has been found to enable for greater separation between the communication waveforms and thereby provides a lower symbol error rate.

### III. FORWARD SCATTERING AT THE TAG

We shall first consider the generation of the communication waveforms at the tag when in the presence of forward scatter effects (*i.e.* multipath). Differences in the forward scattering effects experienced by the tag and the intended receiver could lead to mismatched communication waveforms. For the sake of simplicity we consider the case where multipath-induced mismatch is caused by severe multipath at the tag while the intended receiver (here presumed to be the radar) possesses the actual transmitted radar waveform.

To examine the effects of severe forward scattering at the tag, a random multipath profile is generated as

$$h(t) = \rho_0 \delta(t) + \sum_{\ell=1}^{L-1} \rho_\ell \delta(t - \tau_\ell) \quad (2)$$

where  $\rho_0$  and  $\rho_\ell$  for  $\ell=1, \dots, L$  are i.i.d. complex Gaussian random variables,  $\tau_\ell$  for  $\ell=1, \dots, L$  is uniformly distributed over  $(0, \tau_{\max}]$ , and  $\delta(\bullet)$  is the Dirac delta function. The multipath distorted version of the incident radar waveform at the tag is thus

$$\tilde{s}(t) = s(t) * h(t) \quad (3)$$

where  $*$  is the convolution operation. Note that, in an effort to assess a worst-case scenario, the expected power of the direct path component (the first term in (2)) will be set to be the same as that used for each of the delayed multipath components. Also, the total number of multipath components  $L$  is set to  $NM$  (*i.e.* the dimensionality of the over-sampled

version of the true radar waveform) and  $\tau_{\max}$  is set to the pulse width of the radar waveform (thereby potentially doubling the temporal extent of the presumed incident radar waveform at the tag).

To simulate the effects of multipath distortion a new random multipath profile is independently generated for each run of a Monte Carlo simulation with the resulting  $\tilde{s}(t)$  from (3) being used in (1) to generate the communication waveforms at the tag. One of these waveforms is subsequently embedded in complex Gaussian clutter and attempted to be recovered at the desired receiver. Under the assumption that the receiver is synchronized with the tag (relaxation of this assumption will be addressed elsewhere), Fig. 1 illustrates the probability of symbol error as a function of SNR for each of the three waveform design strategies both for no multipath and severe multipath (with an LFM radar waveform,  $N=100$ ,  $M=2$ , and  $K=4$ ). It is observed that while the Eigenvectors-as-Waveforms and Weighted Combining approaches essentially fail under multipath conditions, the Dominant Projection approach suffers very little performance degradation.

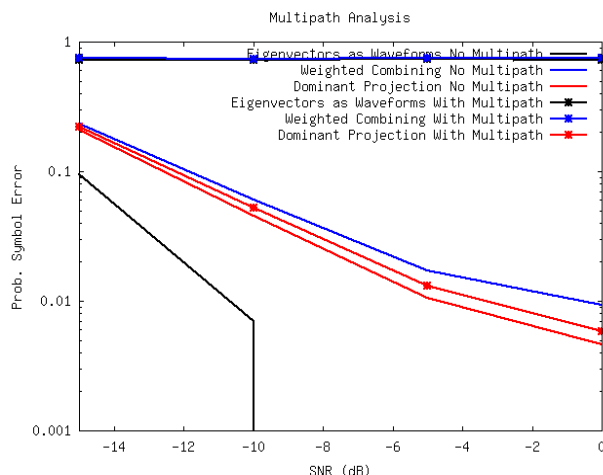


Figure 1. Effect of multipath on each method of generating the communication waveforms.

To understand why the Dominant Projection is robust to multipath while the other two approaches fail, we must examine the way in which the respective eigenvectors are utilized and how the eigenvectors are affected by multipath. In the absence of noise we may express the local scattering as

$$y(t) = s(t) * x(t), \quad (4)$$

where  $x(t)$  is the impulse response representing the radar-illuminated range profile. It is thus observed that (3) and (4) are identical operations. If the multipath-distorted radar waveform  $\tilde{s}(t)$  from (3) is substituted in for the radar waveform  $s(t)$  in (4), the result can be expressed as

$$y(t) = \tilde{s}(t) * x(t) = s(t) * h(t) * x(t) = s * \hat{x}(t) \quad (5)$$

where  $\hat{x}(t) = h(t) * x(t)$  simply corresponds to a different illuminated impulse response. In other words, the multipath distortion of the radar waveform incident upon the tag can be viewed as possessing the same mathematical structure as local ambient scattering, the generic structure of which is employed to design the communication waveforms. However, while it is observed from (5) that multipath and ambient scattering are identical effects that could be combined, this does not yet explain why the Dominant Projection approach is barely affected by multipath while Eigenvectors-as-Waveforms and Weighted Combining fail under multipath conditions. To understand the difference, we must compare the eigenvectors for the cases of with and without multipath.

As an example we again consider an LFM waveform with  $N=100$  and  $M=2$ . Likewise, the multipath profile is again set to have  $\tau_{\max}$  equal to the pulse width to model severe multipath. Thus, a sampled multipath profile vector  $\mathbf{h}$  is modeled as a length  $NM+1$  complex Gaussian vector of i.i.d. components so that  $\tilde{\mathbf{s}}$  (the sampled version of  $\tilde{s}(t)$  from (3)) is a length  $2NM$  vector. Inserting the multipath-distorted radar waveform  $\tilde{\mathbf{s}}$  into (1) to form the matrix  $\tilde{\mathbf{S}}$ , the eigenvectors of  $\tilde{\mathbf{S}}\tilde{\mathbf{S}}^H$  are obtained and denoted as the matrix  $\tilde{\mathbf{V}}$ . For ease of illustration the true radar waveform  $\mathbf{s}$  is appended with  $NM$  zeros such that the result has the same length as  $\tilde{\mathbf{s}}$ . Inserting this zero-padded waveform into (1), the eigenvectors resulting from the correlation matrix are denoted as  $\mathbf{V}$ . Figure 2 depicts an intensity plot (in dB) for the correlation between these two sets of eigenvectors, which is computed as  $|\tilde{\mathbf{V}}^H \mathbf{V}|$ .

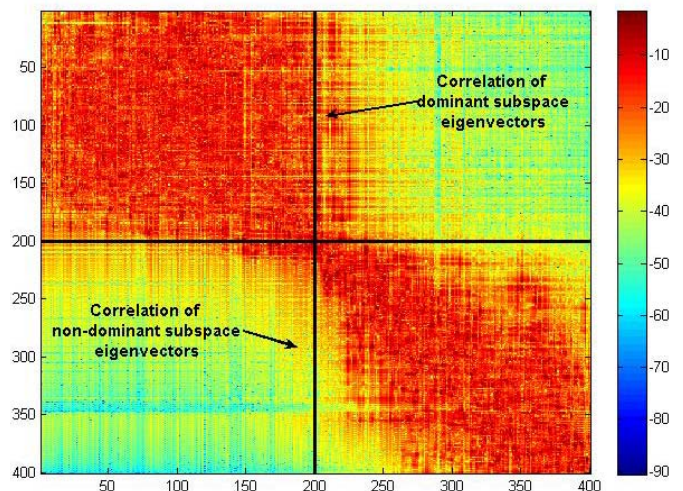


Figure 2. Intensity plot (in dB) of correlations between eigenvector sets formed with and without multipath

Two important observations can be made from Fig. 2. First, despite the presence of multipath the dominant and non-

dominant subspaces (akin to the “signal” and “noise” subspaces, respectively) still remain almost completely separate. Intuitively, this makes sense based on (5) as multipath and ambient scattering are identical operations from a phenomenological perspective and thus should produce similar “signal” and “noise” subspaces. If the respective eigenvector sets are partitioned into dominant and non-dominant sets as  $\tilde{\mathbf{V}}_D$ ,  $\mathbf{V}_D$  and  $\tilde{\mathbf{V}}_{ND}$ ,  $\mathbf{V}_{ND}$ , respectively, (where  $\tilde{\mathbf{V}}_{ND}$  is the orthogonal complement of  $\tilde{\mathbf{V}}_D$  and likewise for  $\mathbf{V}_{ND}$  and  $\mathbf{V}_D$ ) then from this observation of Fig. 2 we can infer that

$$\text{span}\{\tilde{\mathbf{V}}_D\} \approx \text{span}\{\mathbf{V}_D\} \quad (6)$$

and

$$\text{span}\{\tilde{\mathbf{V}}_{ND}\} \approx \text{span}\{\mathbf{V}_{ND}\}. \quad (7)$$

For intra-pulse modulation this means that the ambient scattering interference characterized by the dominant subspace (or alternatively the absence of interference characterized by the non-dominant subspace) can be exploited for communication waveform design regardless of multipath effects.

However, a second observation from Fig. 2 reveals why the Eigenvectors-as-Waveforms and Weighted Combining approaches fail under multipath conditions. It is noted that while the subspaces remain separate, the eigenvectors within a respective subspace are greatly affected by multipath as evidenced by the “smearing” observed within each subspace. As such, we may also infer that  $\tilde{\mathbf{V}}_D \neq \mathbf{V}_D$  and  $\tilde{\mathbf{V}}_{ND} \neq \mathbf{V}_{ND}$ . As a result, any use of individual eigenvectors, such as is done for Eigenvectors-as-Waveforms and Weighted Combining which use particular eigenvectors either directly as communication waveforms or in some pre-determined combination to form the communication waveforms, may not yield a tenable design approach. Note, though, that the Dominant Projection approach [6, 7] relies on the dominant subspace as a whole, which is why very little performance degradation is observed in Fig. 1.

#### IV. TEMPORAL EXPANSION

We now consider the impact of higher dimensionality in the time domain upon communication waveform design. An original premise [6, 7] was that the incident radar waveform is over-sampled by a factor  $M$  relative to the Nyquist bandwidth  $B$ . We will denote the extra bandwidth due to oversampling as  $\Delta B = MB - B$ . It has been observed that higher values of  $\Delta B$  result in a larger non-dominant subspace within which the communication waveforms may reside thereby predicating either higher data rate (via a larger symbol alphabet  $K$ ) or lower receiver symbol error rate. Of course, a larger value of  $\Delta B$  may also increase the intercept probability

as the embedded waveforms can deviate further (in a spectral sense) from the ambient radar scattering.

If one denotes the pulse width of the radar waveform as  $T$ , then a notional illustration of the pulse width  $T$  and bandwidth  $B$  of the incident radar waveform can be illustrated by the *red* region in Fig. 3. As is commonly expressed, the time-bandwidth product for the radar waveform is thus  $B \cdot T$  which is a measure of “dimensionality” for the radar waveform and is used as a measure of the receiver “processing gain”. In the same manner, the dimensionality for the original intra-pulse modulation methods (relying solely on bandwidth expansion) could be expressed, according to the left side of Fig. 3, as  $\Delta B \cdot T$  which is analogous to the dimensionality of the non-dominant subspace.

Let us now consider the impact of temporal (or timewidth) expansion, which we shall denote as  $\Delta T$ . If, instead of bandwidth expansion, one attempts to employ only timewidth expansion a non-dominant subspace will not exist because the ambient scattering resides within the bandwidth  $B$  over all delays of interest. This is depicted as the *orange* region in Fig. 3, which, like the *red* region, is not amenable to the injection of the covert signals because they would be insufficiently discernible from the ambient scattering interference. However, if both bandwidth and timewidth expansion are used, then an additional region of dimensionality  $\Delta B \cdot \Delta T$  is realized that is amenable to embedding a covert communication signal. Thus the total dimensionality for the embedded signal (akin to the processing gain for the embedded signal) is  $\Delta B \cdot (T + \Delta T)$ . From this we may conclude that, while  $\Delta B \rightarrow 0$  is not feasible, the bandwidth expansion may be reduced with no performance penalty if properly compensated for by an expanded timewidth within the communication waveform design framework.

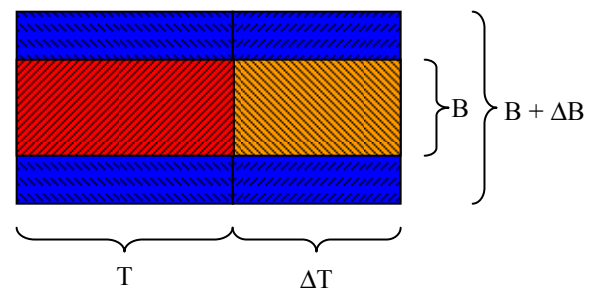


Figure 3. Illustration of the expansion of timewidth and bandwidth of the ambient radar scattering.

As an example, for an LFM radar waveform using  $K = 4$ ,  $N = 100$ , and  $M = 2$  (i.e.  $\Delta B/B = 1$ ) we consider the probability of symbol error for  $\Delta T/T = 0, 0.1, 0.3$ , and  $0.5$  when employing Dominant Projection waveform design and interference cancellation in the desired receiver [7] (no multipath is present in this case). Figure 4 illustrates the results when the expanded timewidth and with no change in

the amount of expanded bandwidth (via over-sampling). Note that even a relatively small increase in timewidth yields a marked benefit in terms of symbol error rate. For example, for an SNR of  $-12$  dB, an increase of  $\Delta T/T$  from 0 to 0.5 yields an order of magnitude reduction in symbol error rate.

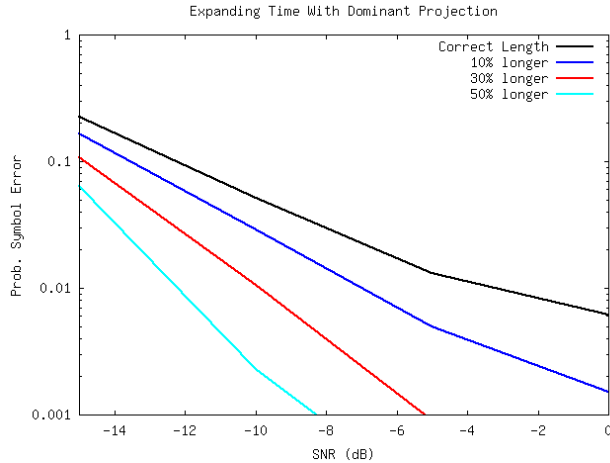


Figure 4. Probability of symbol error for Dominant Projection when exploiting timewidth expansion.

To determine the tradeoff between increasing timewidth versus increasing bandwidth, Monte Carlo simulations were run to compute the symbol error rate (SER) for various  $\Delta B$  and  $\Delta T$ . Figure 5 shows iso-SER curves for the percentage increase in timewidth ( $\Delta T/T$ ) versus percentage increase in bandwidth ( $\Delta B/B$ ). Examination of the iso-SER curves for this scenario reveals that the expected rule-of-thumb relationship

$$\Delta B \cdot (T + \Delta T) = \text{constant} \quad (8)$$

appears to be satisfied. Due to the fact that embedded signal essentially “hides” in the proximity of the ambient scattering, it is expected that reducing  $\Delta B/B$  in return for a commensurate increase in  $\Delta T/T$  will yield enhanced LPI performance. Consider the application of the rule-of-thumb in (8) to determine how much  $\Delta T/T$  must increase given a prescribed decrease in  $\Delta B/B$  so as to maintain a constant symbol error rate. Given some specified  $(\Delta B)_1/B$  to achieve a desired SER and  $(\Delta T)_1/T = 0$ , it can be readily shown that to reduce the expanded bandwidth to some  $(\Delta B)_2/B$  without increasing SER necessitates

$$(\Delta T)_2 = T \left[ \frac{(\Delta B)_1}{(\Delta B)_2} - 1 \right]. \quad (9)$$

Further work is needed to determine if this relationship holds when in the presence of multipath.

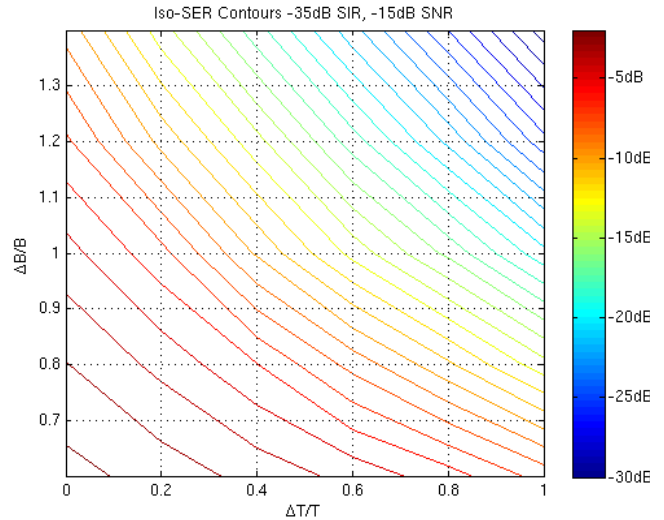


Figure 5. Iso-SER contours for timewidth expansion versus bandwidth expansion.

## V. CONCLUSIONS

The presence of multipath may adversely affect the performance for intra-pulse modulated radar-embedded communications by altering the eigenstructure presumed to represent the local ambient scattering. It has been observed that multipath induces little interaction between the dominant and non-dominant eigensubspaces yet significantly alters the specific eigenvectors within each subspace. As a result, a robust communication waveform design approach should only rely on the subspaces “as a whole” and not specifically utilize individual eigenvectors. In addition, it has been shown that temporal expansion can be used (to some degree) as a surrogate for bandwidth expansion.

## REFERENCES

- [1] R.M. Axline, G.R. Sloan, and R.E. Spalding, “Radar transponder apparatus and signal processing technique,” US Patent #5,486,830, issued Jan. 23, 1996.
- [2] D. Hounam and K.H. Wagel, “A technique for the identification and localization of SAR targets using encoding transponders,” *IEEE Trans. Geoscience & Remote Sensing*, vol. 39, no. 1, pp. 3-7, Jan. 2001.
- [3] D.L. Richardson, S.A. Stratmoen, G.A. Bendor, H.E. Lee, and M.J. Decker, “Tag communication protocol and system,” US Patent #6,329,944, issued Dec. 11, 2001.
- [4] R.C. Ormesher and R.M. Axline, “Methods and system for suppressing clutter in a gain-block, radar-responsive tag system,” US Patent #7,030,805, issued Apr. 18, 2006.
- [5] J.J. Komiak, D.A. Barnum, D.E. Maron, “Digital RF tag,” US Patent #7,106,245, issued Sept. 12, 2006.
- [6] S.D. Blunt and P. Yatham, “Waveform design for radar-embedded communications,” 3<sup>rd</sup> International Waveform Diversity and Design Conference, pp. 214-218, Pisa, Italy, June 4-8, 2007.
- [7] S.D. Blunt, P. Yatham, and J. Stiles, “Intra-pulse radar embedded communications,” to appear in *IEEE Trans. Aerospace & Electronic System*.